Phase-Sensitive Evidence for d-Wave Pairing Symmetry in Electron-Doped Cuprate Superconductors

C. C. Tsuei and J. R. Kirtley

IBM T. J. Watson Research Center, P.O. Box 218, Yorktown Heights, New York 10598

(Received 22 February 2000)

We present phase-sensitive evidence that the electron-doped cuprates $Nd_{1.85}Ce_{0.15}CuO_{4-y}$ (NCCO) and $Pr_{1.85}Ce_{0.15}CuO_{4-y}$ (PCCO) have d-wave pairing symmetry. This evidence was obtained by observing the half-flux quantum effect, using a scanning SQUID microscope, in c-axis-oriented films of NCCO or PCCO epitaxially grown on tricrystal [100] $SrTiO_3$ substrates designed to be frustrated for a $d_{x^2-y^2}$ order parameter. Samples with two other configurations, designed to be unfrustrated for a d-wave superconductor, do not show the half-flux quantum effect.

PACS numbers: 74.20.Mn, 74.50.+r, 74.72.Jt

The intense debate over pairing symmetry in the hole-doped cuprates has been resolved, largely through the development of phase-sensitive symmetry tests, in favor of predominantly d-wave orbital order parameter symmetry for a number of optimally hole-doped high-T_c superconductors [1]. However, the symmetry of the superconducting pair state in the electron-doped cuprates remains controversial. In this Letter, we present a series of phase-sensitive tricrystal experiments as evidence for d-wave pairing in two electron-doped cuprate superconductors [2,3] $Nd_{1.85}Ce_{0.15}CuO_{4-y}$ (NCCO) and $Pr_{1.85}Ce_{0.15}CuO_{4-y}$ (PCCO).

The electron-doped cuprate superconductors ($Ln_{2-x}Ce_xCuO_{4-y}$, Ln = Nd, Pr, Eu, or Sm; $y \simeq 0.04$) are significantly different from their hole-doped counterparts: The hole-doped cuprates such as $La_{2-x}Sr_xCuO_4$ (LSCO) and $YBa_2Cu_3O_7$ (YBCO) have apical oxygen atoms; the electron-doped cuprates do not. Superconductivity in electron-doped cuprate systems occurs in a very narrow doping range ($0.14 \leq x \leq 0.17$ for NCCO [2] and $0.13 < x < 0.2$ for PCCO [3,4]); in the hole-doped LSCO system the range is broader ($0.05 < x < 0.3$). The highest T_c values in the hole-doped cuprates are over 5 times those in the highest T_c electron-doped cuprate systems. In optimally doped YBCO and LSCO the in-plane resistivity increases linearly with temperature over a wide range [5], with small or nearly zero extrapolated values at zero temperature; in PCCO and NCCO ($x = 0.15$) the in-plane resistivity is quadratic in temperature, with a relatively large residual resistivity [4,6]. Photoemission spectroscopy studies show CuO_2 derived flat energy bands near the Fermi surface (FS) of the high-T_c hole-doped cuprates such as YBCO [7] and BSCCO [8], but not within 300 meV of the FS of NCCO [9]. Other physical properties such as the Hall coefficient, thermopower, and the pressure dependence of T_c [10–12], are also different.

Therefore, the following question naturally arises: *Are the pairing symmetries of the electron- and hole-doped cuprates also different*? It is widely believed that the electron-doped cuprates are s-wave superconductors. For example, the in-plane penetration depth $\lambda_{ab}(T)$ in NCCO can be fit with an exponential temperature dependence [12,13] rather than the power law [14,15] expected for unconventional superconductors with a line of nodes in the gap function. However, the distinction between power law and exponential temperature dependences of λ_{ab} can be subtle. Further, the expected temperature dependence of λ_{ab} can change from T to T^2, depending on the amount of disorder scattering [15], which may be large in the electron-doped cuprates [2,4,6]. The paramagnetism arising from Nd^{3+} ions in NCCO is a further complication [16]. After correction for this effect, a linear temperature dependence is found for NCCO by some [16,17], but not by others [18]. Although there is apparently no need for a similar correction in PCCO, it also shows a quadratic, non-s-wave behavior [17], or a Bardeen-Cooper-Schrieffer s-wave exponential dependence [18]. Although the quasiparticle tunneling conductance spectra for NCCO [18–20] closely resemble those of the d-wave hole-doped cuprates [18–21], the absence of a zero bias conductance peak (ZBCP) in NCCO has been taken as evidence for s-wave pairing symmetry [18,19,21]. However, a ZBCP can be suppressed by disorder [22]. Pair tunneling measurements result in the product of the critical current times the junction normal state resistance (I_cR_N) between 0.5 and 6 μV in Pb/NCCO c-axis-oriented films and single crystals [23], almost 3 orders of magnitude smaller than the 3 mV Ambegaokar-Baratoff limit expected for an s-wave superconductor.

In short, contradictory results for NCCO and PCCO underscore the need for a phase-sensitive experiment [1]. Tricrystal phase-sensitive experiments [24] have established d-wave pairing symmetry for many of the optimally hole-doped cuprate superconductors. However, such experiments are difficult in the electron-doped superconductors because of the difficulty in making grain boundary Josephson junctions with sufficiently large critical currents. As reported in the literature, the critical current density J_c decreases exponentially with increasing grain boundary misorientation angle Θ for all cuprates,

 0031-9007/00/85(1)/182(4)$15.00

and can be described by the generic formula [25],

$$J_c(\Theta) = C_i e^{-\Theta/\Theta_i}, \quad (1)$$

where $C_i \sim 4.4 \times 10^7$ A/cm^2 and $\Theta_i \approx 5°$ for hole-doped superconductors, and $C_i \sim 1.8 \times 10^6$ A/cm^2 and $\Theta_i \approx 2°$ for electron-doped superconductors. Despite a similar angular dependence, the J_c values can differ widely between electron- and hole-doped cuprates, especially for high-Θ grain boundary junctions. The original tricrystal configuration [Fig. 1(a)] [24], requires [001] tilt grain boundary junctions with 30° misorientation. According to Eq. (1), J_c for $\Theta = 30°$ should be about 0.5 A/cm^2 for NCCO, 5 orders of magnitude smaller than for YBCO [24]. Although this disadvantage can be partially offset by making thicker films, care must be taken to avoid film inhomogeneity and retain film epitaxy. With these constraints in mind, we have deposited c-axis-oriented epitaxial films (thickness ~6000–10 000 Å) of NCCO and PCCO on various tricrystal [100] $SrTiO_3$ substrates. The electron-doped cuprate films were grown epitaxially on the substrate at $T = 750$ °C using pulsed laser deposition from a stoichiometric target of NCCO or PCCO in 300 mTorr of nitrous oxide. The film deposition is followed by a vaccum annealing at 750 °C for 5 minutes followed by a slow cooling to room temperature. This achieves a full oxygenation during film growth, followed by a controlled reduction to remove the excess oxygen at the apical site (i.e., in $Nd_{1.85}Ce_{0.15}CuO_{4-y}$, $y \simeq 0.04$).

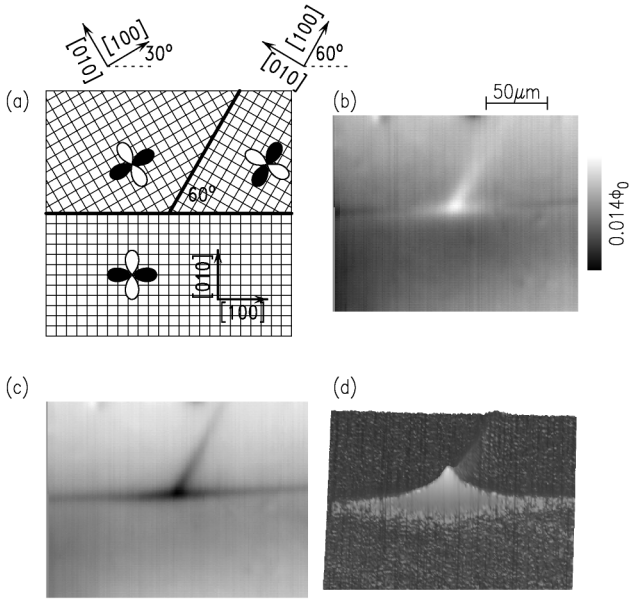

FIG. 1. (a) Geometry of the frustrated tricrystal geometry, with polar plots of the pairing orbital wave functions (white and black indicating opposite signs) for a $d_{x^2-y^2}$ superconductor. (b), (c) SSM images of a NCCO thin film epitaxially grown on the STO substrate (a), cooled in nominal zero field and imaged at 4.2 K with a square pickup loop 7.5 μm in diameter, with fields of +0.2 mG (b) and −0.2 mG (c) applied. (d) A three-dimensional rendering of the image [(b) − (c)]/2.

A judicious control of the oxygen content is crucial for maximizing T_c, and to control other superconducting and normal-state properties in the bulk and at the junction interface [26].

Our films have a T_c of 22–25 K for NCCO, and 22–23 K for PCCO. The 10%–90% resistive transition width is 0.6 K or less. The in-plane normal-state resistivity is ~300 $\mu\Omega$ cm at room temperature, with a quadratic temperature variation [6]. The room temperature to T_c resistivity ratio is 5 to 6. The critical current of an NCCO bicrystal grain boundary junction ($\Theta = 30°$) at 4.2 K and ambient magnetic field is $J_c = 6 \pm 2$ A/cm^2, about a factor of 10 larger than predicted by Eq. (1), indicating better sample quality.

As in the previous tricrystal experiments [1,24], we use a scanning SQUID microscope (SSM) [27] to measure the magnetic fields near the tricrystal point of a c-axis-oriented epitaxial cuprate film deposited on a tricrystal (100) $SrTiO_3$ type orbital (STO) substrate [Fig. 1(a)]. The crystallographic orientations of the tricrystal were chosen to form an energetically frustrated state at the tricrystal point for a superconductor with $d_{x^2-y^2}$ pairing symmetry, regardless of whether the grain boundary junction interface is in the clean or dirty limit [24]. This frustration is relaxed by the spontaneous generation of a magnetic vortex with total flux Φ being half of the conventional superconductor flux quantum ($\Phi = \Phi_0/2 = hc/4e$). Direct observation of this half-flux quantum effect serves as conclusive evidence for d-wave symmetry. Shown in Figs. 1(b) and 1(c) are SSM images for an NCCO film deposited on an STO substrate with the geometry of Fig. 1(a). These images are of Josephson vortices with fields either pointing out of (b) or into (c) the sample, centered at the tricrystal point and extending along the grain boundaries. The images are complicated by smooth variations in the background signal, inductive interactions between the SQUID and the sample, and dipolar features (often observed in SSM images of cuprate superconductors [28]), presumably due to roughness and/or magnetic inhomogeneities at the surface. Figure 1(d) shows a three-dimensional rendering of an image obtained by subtracting (c) from (b) (and dividing by 2). This largely removes the extraneous features. There are several evidences that the magnetic signals at the tricrystal point are due to half-flux quantum Josephson vortices. First, although the vortices can switch signs, the field magnitude is the same after these changes, and there is always a vortex with this general appearance at the tricrystal point, under any conditions of cooldown and externally applied magnetic field. Further, the observed magnetic fields agree with those expected for the half-flux quantum Josephson vortex. The normal component of the magnetic field from such a vortex at the superconducting surface is given by [29]

$$B_z(r_i, r_{i\perp}) = \frac{\Phi_0 a_i}{\pi \lambda_L \lambda_{Ji}} \frac{e^{-r_i/\lambda_{Ji}}}{1 + a_i^2 e^{-2r_i/\lambda_{ji}}} e^{-|r_{i\perp}|/\lambda_L}, \quad (2)$$

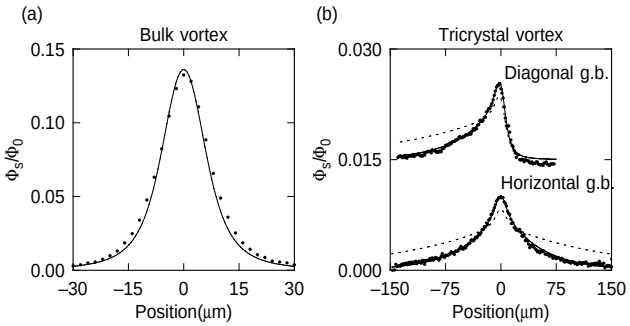

FIG. 2. Cross sections through the SSM image (d) of the sample of Fig. 1. (a) Cross section (solid symbols) and modelling (line, $z = 7.6$ μm) of a bulk vortex. (b) Cross sections through the tricrystal point (solid symbols) parallel to the horizontal and diagonal (offset by $0.015\Phi_0$ for clarity) grain boundaries, and best fits to the fields from a Josephson vortex with total flux $\Phi_0/2$ (solid line, $\lambda_J = 48$ μm) and $\Phi = \Phi_0$ (dashed line, $\lambda_J = 137$ μm).

where r_i is the distance along the ith grain boundary from the tricrystal point, $r_{i\perp}$ is the perpendicular distance from the ith (closest) grain boundary, λ_L is the London penetration depth, λ_{Ji} is the Josephson penetration depth of the ith grain boundary, and the a_i's are normalization constants chosen such that the magnetic field is continuous at the tricrystal point and the total flux in the vortex is equal to $\Phi_0/2 = hc/4e$. The pickup loop is a distance z above, and nearly parallel to, the surface of the sample. The distance z is determined by fitting data for an isolated Abrikosov vortex to the fields $B_z = (\Phi_0/2\pi)z/|r|^3$, integrating over the known area of the pickup loop, with z as the sole fitting parameter [see Fig. 2(a)]. The fields calculated from Eq. (2) are propagated above the surface [29] by this height z and integrated over the SQUID pickup loop for comparison with experiments. An example is shown in Fig. 2(b). In this figure the solid points are cross sections through the SSM image of Fig. 1(d) through the tricrystal point and parallel to the horizontal and diagonal grain boundaries. The lines are fits to this data, using the Josephson penetration depth as the sole fitting parameter. The solid line assumes $\Phi = \Phi_0/2$ and the dashed line is the best fit for $\Phi = \Phi_0$. If we vary Φ while optimizing the Josephson penetration depths, we find $\Phi = (0.47 + 0.18 - 0.14)\Phi_0$, using a doubling of the best fit χ^2 values as the criterion for assigning error bars. The value for λ_J found from this fit assuming $\Phi = \Phi_0/2$ is 48 μm, corresponding to $J_c = \hbar c^2/8\pi e d\lambda_J^2 \sim 20$ A/cm^2 (taking $d = 2\lambda_{ab} = 0.5$ μm). Comparison of the value for J_c obtained in this way for another tricrystal sample was in good agreement with a 4-point probe measurement on a bicrystal grain boundary junction fabricated at the same time. We obtained qualitatively similar results on repeated measurements of five NCCO samples with the same (frustrated) geometry.

We repeated these experiments with tricrystal NCCO films in two different unfrustrated configurations

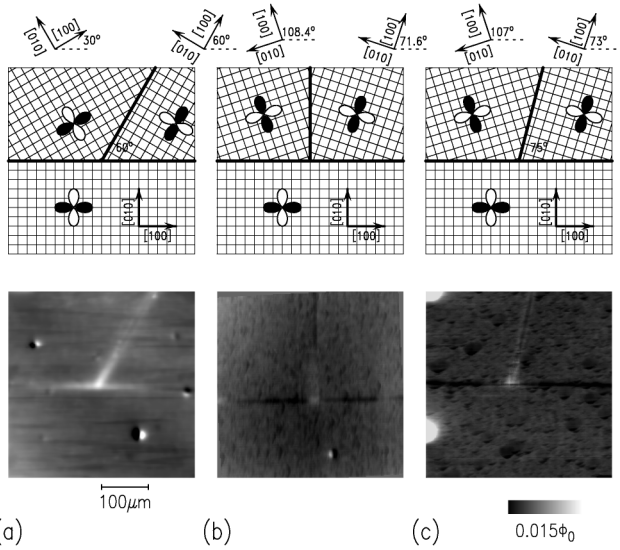

FIG. 3. SSM images, centered at the tricrystal points, of NCCO samples with three different geometries (shown schematically). The samples were cooled in nominal zero field and imaged at 4.2 K with an octagonal pickup loop 10 μm in diameter. The sample with a geometry designed to be frustrated for a $d_{x^2-y^2}$ superconductor (a) shows the half-flux quantum effect. Samples with two other geometries (b), (c), designed to be unfrustrated for a $d_{x^2-y^2}$ superconductor, do not.

[Figs. 3(b) and 3(c)] designed *not* to show the half-flux quantum effect if NCCO *is* a d-wave superconductor. SSM images from samples in all three geometries are presented in Fig. 3. Figure 3(c) shows fringing fields from two Abrikosov vortices just outside the scan area. The samples in the nonfrustrated geometries show little, if any, flux at the tricrystal points. There is a residual signal at the grain boundaries and the tricrystal point, which may be due to topographic effects, faceting [30], or small changes in the mutual inductance between the SQUID and sample. Even if we attribute the signal at the tricrystal point in the unfrustrated samples to magnetic fields trapped in the grain boundaries, the total magnetic flux is less than a few percent of the flux seen at the tricrystal point in the frustrated sample. We therefore conclude that the frustrated sample [Fig. 3(a)] shows the half-flux quantum effect, while the other two samples [Figs. 3(b) and 3(c)] do not. This is consistent with NCCO being a $d_{x^2-y^2}$ superconductor.

Similar results have been obtained in a second electron-doped cuprate, PCCO. Figure 4 shows scanning SQUID microscope images of a PCCO film epitaxially grown on a STO substrate with the frustrated geometry of Fig. 1(a). A half-flux quantum Josephson vortex [Fig. 4(a)] was spontaneously generated at the tricrystal point, and could be inverted [Fig. 4(b)] by varying the external field. The difference image $[(a) - (b)]/2$ could be well fit to Eq. (2), assuming $\Phi = \Phi_0/2$, indicating that PCCO has predominantly d-wave pairing symmetry. Further, sum images $[(a) + (b)]/2$ [e.g., Fig. 4(c)] showed almost no feature at

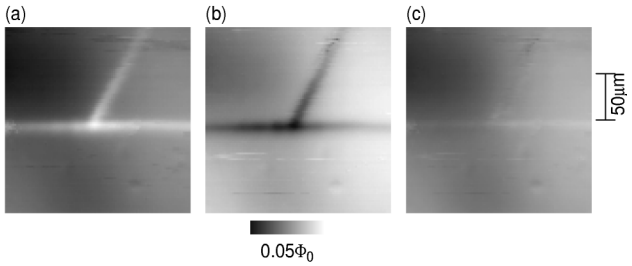

FIG. 4. SSM images of a PCCO frustrated tricrystal sample, cooled in nominal zero field and imaged at 4.2 K with a square pickup loop 7.5 μm on a side, with applied field of +0.2 mG (a) and −0.2 mG (b). The featureless sum image (c), = [(a) + (b)]/2, indicates time-reversal invariance.

the tricrystal point in both NCCO and PCCO. This indicates that time-reversal invariance is obeyed in the pairing in the electron-doped cuprates.

In conclusion, we have used a scanning SQUID microscope in a series of tricrystal experiments to produce definitive phase-sensitive evidence for d-wave pairing symmetry in the electron-doped cuprate superconductors NCCO and PCCO. Thus predominantly d-wave superconductivity is established in both optimally electron- and hole-doped high-T_c superconductors. This is consistent with several previously thought anomalous experimental observations. For example, the extremely small I_cR_N product for c-axis pair tunneling in Pb/NCCO junctions [23] is in accordance with a predominantly d-wave order parameter in NCCO. The small and finite I_cR_N product may be due to symmetry-broken-induced s-wave pairing at the junction interface or other extrinsic mechanisms. The missing ZBCP in the NCCO quasiparticle conductance spectra may well be due to strong scattering effects. Finally, the power-law temperature dependence observed in some $\lambda_{ab}(T)$ data supports our conclusion that both NCCO and PCCO are d-wave superconductors.

We are grateful to A. Gupta, R.H. Koch, J. Mannhart, K.A. Moler, D.M. Newns, J.Z. Sun, and S.I. Woods for useful discussions, and G. Trafas for technical assistance.

[1] D. J. Scalapino, Phys. Rep. **250**, 329 (1995); J. F. Annett, N. D. Goldenfeld, and A. J. Leggett in *Physical Properties of High Temperature Superconductors V,* edited by D. M. Ginsberg (World Scientific, Singapore, 1996), Chap. 6, p. 376; C. C. Tsuei and J. R. Kirtley, Rev. Mod. Phys. (to be published).

[2] Y. Tokura, H. Takagi, and S. Uchida, Nature (London) **337**, 345 (1989).

[3] H. Takagi, S. Uchida, and Y. Tokura, Phys. Rev. Lett. **62**, 1197 (1989).

[4] J. L. Peng, E. Maiser, T. Venkatesan, R. L. Greene, and G. Czjzek, Phys. Rev. B **55**, R6145 (1997).

[5] H. Takagi *et al.,* Phys. Rev. Lett. **69**, 2975 (1992).

[6] C. C. Tsuei, A. Gupta, and G. Koren, Physica (Amsterdam), **161C**, 415 (1989).

[7] A. A. Abrikosov, J. C. Campuzano, and K. Gofron, Physica (Amsterdam) **214C**, 73 (1993).

[8] D. S. Dessau *et al.,* Phys. Rev. Lett. **71**, 2781 (1993).

[9] D. M. King *et al.,* Phys. Rev. Lett. **70**, 3159 (1993).

[10] H. Kontani, K. Kanki, and K. Udea, Phys. Rev. B **59**, 14 723 (1999).

[11] C. Murayama *et al.,* Nature (London) **339**, 292 (1989); J. T. Markert *et al.,* Phys. Rev. Lett. **64**, 80 (1990).

[12] S. M. Anlage *et al.,* Phys. Rev. B **50**, 523 (1994).

[13] D. H. Wu *et al.,* Phys. Rev. Lett. **70**, 85 (1993); A. Andreone *et al.,* Phys. Rev. B **49**, 6392 (1994).

[14] W. N. Hardy *et al.,* Phys. Rev. Lett. **70**, 3999 (1993); D. A. Bonn *et al.,* Phys. Rev. B **50**, 4051 (1994).

[15] J. Annett, N. Goldenfeld, and S. R. Renn, Phys. Rev. B **43**, 2778 (1991); P. J. Hirschfeld and N. Goldenfeld, Phys. Rev. B **48**, 4219 (1993).

[16] J. R. Cooper, Phys. Rev. B **54**, R3753 (1996).

[17] J. D. Kokales *et al.,* cond-mat/0001166; R. Prozorov *et al.,* cond-mat/9912001.

[18] L. Alff *et al.,* Phys. Rev. Lett. **83**, 2644 (1999).

[19] S. Kashiwaya *et al.,* Phys. Rev. B **57**, 8680 (1998).

[20] M. Covington *et al.,* Phys. Rev. Lett. **79**, 277 (1997).

[21] L. Alff *et al.,* Phys. Rev. B **58**, 11 197 (1998).

[22] M. Aprili *et al.,* Phys. Rev. B **57**, R8139 (1998).

[23] S. I. Woods *et al.,* IEEE Trans. Appl. Supercond. **9**, 3917 (1999).

[24] C. C. Tsuei *et al.,* Phys. Rev. Lett. **73**, 593 (1994); J. R. Kirtley *et al.,* Nature (London) **373**, 225 (1995).

[25] H. Hilgenkamp and J. Mannhart, IEEE Trans. Appl. Supercond. **9**, 3405 (1999); U. Schoop *et al., ibid.* **9**, 3409 (1999).

[26] H. Yamamoto, M. Naito, and H. Sato, Phys. Rev. B **56**, 2852 (1997).

[27] J. R. Kirtley *et al.,* Appl. Rev. Lett. **66**, 1138 (1995).

[28] A preliminary SSM study as a function of temperature for $T = 4.2$ K to 30 K shows that these small features persist above T_c.

[29] J. R. Kirtley *et al.,* Phys. Rev. Lett. **76**, 1336 (1996).

[30] Although faceting induced sign changes in the pairing wave function can be a complication for, e.g., 45° asymmetric grain boundaries, they are much less common in the 30° grain boundaries used in this study. [See H. Hilgenkamp, J. Mannhart, and B. Mayer, Phys. Rev. B **53**, 14 586 (1996)].